

Electromagnetic response of gravitational waves passing through an alternating magnetic field: A scheme to probe high-frequency gravitational waves

H. Zheng,¹ L. F. Wei,^{1,2,3,*} H. Wen,⁴ and F. Y. Li⁴

¹State Key Laboratory of Optoelectronic Materials and Technologies, School of Physics, Sun Yat-sen University, Guangzhou 510275, China

²Photonics Laboratory and Institute of Functional Materials, College of Science, Donghua University, Shanghai 201620, China

³Information Quantum Technology Laboratory, School of Information Science and Technology, Southwest Jiaotong University, Chengdu 610031, China

⁴Institute of Gravitational Physics and Department of Physics, Chongqing University, Chongqing 400044, China



(Received 15 October 2017; published 14 September 2018)

In principle, gravitational waves could exist at any frequency. Recently, the LIGO-Virgo Collaboration detected gravitational waves (GWs) by probing their *mechanical responses* with laser interferometers. The detected GWs are in the intermediate-frequency band, i.e., GW150914: 35–250 Hz; GW151226: 35–450 Hz; GW170104: 30–350 Hz; GW170814: 35–450 Hz; and GW170817: 30–350 Hz. Alternatively, in this paper we investigate the observable electromagnetic responses (EMRs) of the GWs, passing through an alternating magnetic field. We show that, differing from the original Gertsenshtein-Zeldovich effect (which is the second-order effect of the amplitude of the GW passing through a high stationary magnetic field and consequently is too weak to be detected), the EMRs of the GWs in the present configuration are the first-order perturbation effects and thus the induced perturbation photon fluxes are detectable with the current well-developed weak-light detection techniques. Furthermore, we show that the wave impedances of the GW-induced electromagnetic wave perturbations are very different from those of the background electromagnetic noises (i.e., $\cong 377 \Omega$ for EM radiation in the background flat space-time). Therefore, with a properly designed wave-matching technique, the stronger background EM noise (without any GW information) can be effectively filtered out, and thus only the GW-induced perturbation photon fluxes are conducted to the detectors. The configuration proposed here could be utilized to actively look for GWs in a sufficiently wide frequency band, depending on the achievable scales of the required high magnetic fields. Hopefully, the proposal could provide a platform to detect GWs based on their electromagnetic response in higher frequency bands.

DOI: [10.1103/PhysRevD.98.064028](https://doi.org/10.1103/PhysRevD.98.064028)

I. INTRODUCTION

It is well known that, as a strict and beautiful theory on the interactions of matter, space, and time on large scales, Einstein's general relativity has been supported by a series of astronomical observations and simulation experiments. Interestingly, one of the most important predictions in general relativity—the existence of gravitational waves (GWs), i.e., ripples in the curvature of space-time that propagate as waves at the speed of light [1]—has been verified recently by the LIGO laser interferometers [2–6] via probing the minute mechanical displacements of space-time. The GWs detected recently by the LIGO-Virgo Collaboration [7–9] were in the intermediate-frequency

band, i.e., GW150914: 35–250 Hz; GW151226: 35–450 Hz; GW170104: 30–350 Hz; GW170814: 35–450 Hz; and GW170817: 30–350 Hz. Their peak strains are of the order of 10^{-21} . It was argued that [2] these detected GW signals were caused by the mergers of binary black holes with masses dozens of times that of the Sun about a few billion years ago. In principle, GWs could exist at any frequency [10], and might come from various sources (see, e.g., Refs. [11,12]). Importantly, the detection of GWs at various frequencies could not only provide more evidence to verify Einstein's gravitational theory in a wider frequency band, but also open the era of gravitational-wave astronomy [13,14].

Certainly, the detection or observation of GWs is a great challenge for laboratories on Earth, due to their significantly minute amplitudes. Historically, many approaches

*lfwei@dhu.edu.cn

have been proposed to detect or observe GWs, based on Einstein's prediction. These approaches can be roughly divided into two types: indirect observation and direct detection. In fact, before the recent LIGO-Virgo direct detections, indirect experimental evidence of the existence of GWs was obtained by Hulse and Taylor [15,16] by observing the change in the orbital period of the binary PSR B1913+16 (a pair of stars, one of which is a pulsar). The observed pulsar's signals were used to determine how much energy was radiated in the form of GWs. Accordingly, the orbital period decays at a rate predicted theoretically by the energy loss due to the GW radiation. Also, observing the B-mode polarization in the cosmic microwave background is regarded as another approach to indirectly verify the existence of GWs in very low-frequency band [17]. It is believed that such an observation is further related to the experimental confirmation of the inflationary cosmological model.

The original direct detection experiments involved the use of resonant detectors, typically the famous Weber beam [18]: a system oscillates mechanically at a certain frequency, and the incident GWs induce a mechanical vibration that could be detected. However, this line of thinking has for the most part reached its end point, and improving its sensitivity further seems to be impossible. Since 1980s, laser interferometers—including the current LIGO-Virgo setup [7–9] and the proposed Laser Interferometer Space Antenna (LISA) [19,20] and Einstein telescope [21–23]—have been proposed to directly detect GW-induced mechanical displacements: the incident GWs alter the path length of the interferometer arms and are detected via probing the changing interference patterns. Similarly, pulsar timing and pulsar-timing arrays, which probe the GW-induced change of the path length between the pulsars and Earth via timing a set of pulsars, have been utilized to detect GWs [24,25].

Besides the tidal effects used in the above GW detectors, the electromagnetic responses (EMRs) of the GWs, i.e., the so-called Gertsenshtein-Zel'dovich (GZ) effect [26], could potentially be utilized to detect GWs. The GZ effect describes a mutual electromagnetic wave (EMW)-GW conversion in a high stationary magnetic field. This implies that a GW propagating through a magnetic field yields a stress tensor and compression of the field. As a consequence, an alternating electromagnetic field (i.e., an EMW) with certain information about the passing GWs (typically the relevant metric perturbations) could be generated and detected. Unfortunately, the amplitude of such a GW-induced EMW is too minute to be detected [27], as the relevant detectable quantities (such as the power or photon flux) are proportional to the square of the amplitudes of the passing GWs [28,29]. To overcome such a difficulty, a series of modified schemes have been proposed by introducing certain auxiliary EMWs (including e.g., plane EMWs [30] and Gaussian beams [31]) to enhance the

observable effects of the GW-induced perturbation EMW signals. With them, the observable quantities of the GW-induced EMW signals become linearly dependent on the amplitudes of the passing GWs. However, it is not easy to conduct the desired auxiliary EMWs to the experimental detectors, and the auxiliary EMWs would unavoidably increase noise and consequently decrease the sensitivities of the detectors, in principle.

In this paper, we propose an alternative approach to implement the direct detection of GWs by using the GZ effect with an alternating magnetic field. Differing from the original GZ configuration with only a high stationary magnetic field, in our proposal a relatively weak alternating magnetic field is additionally applied. By exactly solving the relevant Einstein-Maxwell equation in a curved space-time, we show that the EMRs of the GWs in the present configuration are the first-order effects of the passing GWs, i.e., the observable quantities (typically the GW-induced signal photon fluxes) are linear in the amplitudes of the passing GWs. As a consequence, the generated perturbation EMW signals could be detected with the current weak-light detection techniques [32–36]. As the amplitude and the frequency of the applied weak alternating magnetic field are locally controllable, the present scheme could be applied to actively search for GWs in a sufficiently wide frequency band, once the scale of the applied magnetic field is experimentally reachable. Also, our analysis shows that the wave impedances of the GW-induced EMW signals, satisfying the Einstein-Maxwell equation in the curved space-time, are very different from those of the background EM noise (which obey the flat space-time Maxwell equation and thus always take the value of 377Ω in vacuum). As a consequence, by using the well-developed wave-impedance-matching technique [37,38], the background EM noise could be safely filtered out and only the GW-induced EM signals (i.e., the signal photon fluxes) would be left to be conducted into the detectors.

The paper is organized as the follows. In Sec. II, as a typical example we specifically discuss the EM responses of a monochromatic circular polarized plane GW with frequency ω_g passing through an alternating magnetic field, $B_y^{(0)} + B_y' \sin(\omega_B t)$, by exactly solving the Einstein-Maxwell equations. For simplicity, the background EM noise (i.e., background photons) is simply treated as the noise generated by the usual electromagnetic inductions, and the signal photons are related to the curved space-time metric. The strengths of these two kinds of EM signals (e.g., the average photons per second passing through a unit surface) are calculated in detail. The wave impedance matching scheme, i.e., how to filter out the background photons to implement the detection of the pure GW-induced signal photons by the single-photon detector, is described in Sec. III. A preliminary noise analysis in the proposed scheme to probe the electromagnetic responses of

the GWs is also given. Finally, we provide our concluding remarks in Sec. IV.

II. ELECTROMAGNETIC RESPONSE OF THE LOCALLY ALTERNATING MAGNETIC FIELD TO A GRAVITATIONAL WAVE

Without loss of generality and for simplicity, we consider the electromagnetic responses of a monochromatic circular polarized plane GW propagating along the z axis, which can be treated as the perturbed ripples

$$\begin{cases} h_{\oplus} = h_{xx} = -h_{yy} = A_{\oplus}\Lambda_{\omega}(z, t), \\ h_{\otimes} = h_{xy} = h_{yx} = iA_{\otimes}\Lambda_{\omega}(z, t) \end{cases} \quad (1)$$

to the background flat Minkowski space-time. Here, the usual TT gauge is used and $\Lambda_{\omega_g}(z, t) = \exp[i(k_g z - \omega_g t)]$. As a consequence, the curved space-time wherein the GWs propagate can be described by the following metric:

$$g_{\alpha\beta} = \eta_{\alpha\beta} + h_{\alpha\beta} = \begin{bmatrix} 1 & & & \\ & -1 + h_{\oplus} & h_{\otimes} & \\ & h_{\otimes} & -1 - h_{\oplus} & \\ & & & -1 \end{bmatrix}, \quad (2)$$

with

$$\eta_{\alpha\beta} = \begin{bmatrix} 1 & & & \\ & -1 & 0 & \\ & 0 & -1 & \\ & & & -1 \end{bmatrix} \quad (3)$$

being the usual flat Minkowski metric.

Now we consider the configuration shown in Fig. 1, wherein the GWs pass through a background magnetic field $\mathbf{B}(t) = (0, B_y^{(0)} + B'_y \sin(\omega_B t), 0)$ confined in the cavity. $B_y^{(0)}$ is a static magnetic field, and $B'_y(t) = B'_y \sin(\omega_B t)$ with $B'_y < B_y^{(0)}$ is the alternating magnetic field with frequency ω_B . For simplicity, the transmission of cavity photons along the $-z$ direction are neglected. Obviously, the background electromagnetic field tensor in the absence of GWs reads

$$F_{\alpha\beta}^{(0)} = \begin{bmatrix} 0 & & & \\ & 0 & B_y^{(0)} + B'_y \sin(\omega_B t) & \\ & & 0 & \\ -B_y^{(0)} - B'_y \sin(\omega_B t) & & & 0 \end{bmatrix}. \quad (4)$$

In the presence of GWs, the electromagnetic field tensor in the cavity becomes

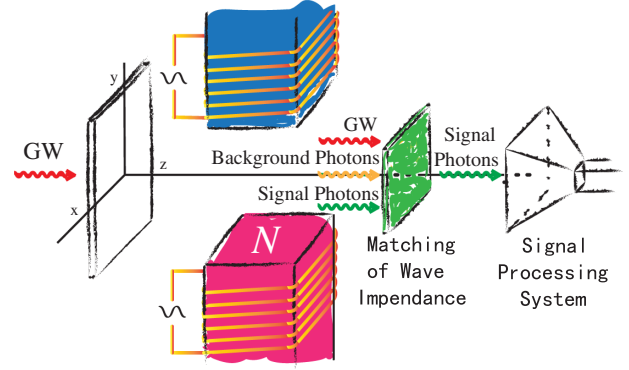


FIG. 1. An experimental configuration to probe the electromagnetic responses of GWs using a single-side transmission cavity (i.e., the photon cannot be transmitted through the left boundary of the cavity). The cavity is biased by an alternating magnetic field $B(t)$. It is assumed that a monochromatic circular polarized plane gravitational wave passes through the cavity along the z axis. Thus, only the signal photon fluxes can pass through the wave-impedance matcher for detection in a signal-processing system.

$$F_{\alpha\beta} = F_{\alpha\beta}^{(0)} + F_{\alpha\beta}^{(1)} = \begin{bmatrix} 0 & \tilde{E}_x & \tilde{E}_y & \tilde{E}_z \\ -\tilde{E}_x & 0 & -\tilde{B}_z & X \\ -\tilde{E}_y & \tilde{B}_z & 0 & -\tilde{B}_x \\ -\tilde{E}_z & -X & \tilde{B}_x & 0 \end{bmatrix}, \quad (5)$$

where $X = B_y^{(0)} + B'_y \sin(\omega_B t) + \tilde{B}_y$, $\vec{E} = (\tilde{E}_x, \tilde{E}_y, \tilde{E}_z)$, and $\vec{B} = (\tilde{B}_x, \tilde{B}_y, \tilde{B}_z)$. With the metric (2), the contravariant form of the above electromagnetic field tensor reads

$$F^{\mu\nu} = \begin{bmatrix} 0 & -\tilde{E}_x & -\tilde{E}_y & -\tilde{E}_z \\ \tilde{E}_x & 0 & -\tilde{B}_z & Y \\ \tilde{E}_y & \tilde{B}_z & 0 & -Z \\ \tilde{E}_z & -Y & Z & 0 \end{bmatrix}, \quad (6)$$

where $Y = [B_y^{(0)} + B'_y \sin(\omega_B t)](1 - h_{\oplus}) + \tilde{B}_y$ and $Z = [B_y^{(0)} + B'_y \sin(\omega_B t)]h_{\otimes} + \tilde{B}_y$. Above, the high-order effects of the GW perturbations have been neglected, as they are very weak.

Physically, the electromagnetic field described by the tensors (5) and (6) obey the relevant Einstein-Maxwell equations,

$$\begin{cases} \partial_{\nu} \sqrt{-g} F^{\mu\nu} = \partial_{\nu} (\sqrt{-g} g^{\mu\alpha} g^{\beta\gamma} F_{\alpha\beta}) = 0, & g = |g_{\alpha\beta}| \\ \partial_{\alpha} F_{\beta\gamma} = 0. \end{cases} \quad (7)$$

Formally, these covariant differential equations can be specifically decomposed into the following equations with the usual differentials defined in the flat space-time:

$$\begin{aligned} \frac{1}{c^2} \partial_t^2 \tilde{E}_x - \partial_z^2 \tilde{E}_x &= A_{\oplus} B_y^{(0)} k_g \omega_g \Lambda_{\omega_g}(z, t) \\ &\quad - \frac{i}{2} A_{\oplus} B_y' k_g \Delta_- \exp[i(k_g z - \Delta_- t)] \\ &\quad + \frac{i}{2} A_{\oplus} B_y' k_g \Delta_+ \exp[i(k_g z - \Delta_+ t)], \end{aligned} \quad (8)$$

$$\begin{aligned} \frac{1}{c^2} \partial_t^2 \tilde{B}_y - \partial_z^2 \tilde{B}_y &= A_{\oplus} B_y^{(0)} k_g \omega_g \Lambda_{\omega_g}(z, t) \\ &\quad - \frac{i}{2} A_{\oplus} B_y' k_g^2 \exp[i(k_g z - i\Delta_- t)] \\ &\quad + \frac{i}{2} A_{\oplus} B_y' k_g^2 \exp[i(k_g z - i\Delta_+ t)] \\ &\quad + \frac{1}{c^2} \omega_B^2 B_y' \sin(\omega_B t), \end{aligned} \quad (9)$$

with $\Delta_+ = \omega_g + \omega_B$ and $\Delta_- = \omega_g - \omega_B$.

As one can see, the \oplus and \otimes polarizations of the gravitational wave modulate the x/y and y/x polarizations of the signal electromagnetic wave, respectively. Let us specifically discuss the \oplus polarization modulations (the \otimes polarization modulations can also be treated similarly). For convenience, we decompose the solutions of Eqs. (8) and (9) into three parts, i.e.,

$$\begin{cases} \tilde{E}_x(z, t) = \tilde{E}_x^{(0)}(z, t) + \tilde{E}_x^{(1)}(z, t) + \tilde{E}_x^{\prime(1)}(z, t), \\ \tilde{B}_y(z, t) = \tilde{B}_y^{(0)}(z, t) + \tilde{B}_y^{(1)}(z, t) + \tilde{B}_y^{\prime(1)}(z, t). \end{cases} \quad (10)$$

The zeroth-order solutions

$$\begin{aligned} \tilde{E}_x^{(0)}(z, t) &= -\frac{B_y' c}{2} \sin\left(\frac{\omega_B z}{c} - (\omega_B t)\right), \\ \tilde{B}_y^{(0)}(z, t) &= \frac{\tilde{E}_x^{(0)}(z, t)}{c} \end{aligned} \quad (11)$$

describe the usual electromagnetic inductions without the GW perturbation. The first-order ones are originated from the perturbations of the passing GWs, where

$$\begin{aligned} \tilde{E}_x^{(1)} &= \frac{i}{2} A_{\oplus} B_y^{(0)} \omega_g z \Lambda_{\omega_g}(z, t) \\ &\quad + A_1 \Lambda_{\omega_g}(z, t) + A_2 \Lambda_{-\omega_g}(z, t), \\ \tilde{B}_y^{(1)} &= \frac{i}{2} A_{\oplus} B_y^{(0)} k_g z \Lambda_{\omega_g}(z, t) \\ &\quad + A_1 \Lambda_{\omega_g}(z, t) + A_2 \Lambda_{-\omega_g}(z, t), \end{aligned} \quad (12)$$

(with $\Lambda_{\mp\omega_g}(z, t) = \exp[i(k_g z \pm \omega_g t)]$) describe the effects of the GWs perturbing the stationary magnetic field $B_y^{(0)}$ [26], and

$$\begin{aligned} \tilde{E}_x^{\prime(1)} &= i \sum_{\alpha=-,+} \alpha \Phi_{\alpha} \exp[i(k_g z - \Delta_{\alpha} t)] \\ &\quad + \sum_{\alpha=-,+} \{C_{\alpha} \Lambda_{\Delta_{\alpha}}(z, t) + D_{\alpha} \Lambda_{-\Delta_{\alpha}}(z, t)\}, \\ \tilde{B}_y^{\prime(1)} &= i \sum_{\alpha=-,+} \alpha \Psi_{\alpha} \exp[i(k_g z - \Delta_{\alpha} t)] \\ &\quad + \sum_{\alpha=-,+} \{E_{\alpha} \Lambda_{\Delta_{\alpha}}(z, t) + F_{\alpha} \Lambda_{-\Delta_{\alpha}}(z, t)\}, \end{aligned} \quad (13)$$

(with $\Lambda_{\mp\Delta_{\alpha}}(z, t) = \exp[i\Delta_{\alpha}(z/c \pm t)]$) are due to the GW perturbations of the applied alternating magnetic field with amplitude B_y' . Above,

$$\Phi_{\pm} = \frac{A_{\oplus} B_y' \omega_g \Delta_{\pm} c}{2[\omega_g^2 - \Delta_{\pm}^2]}, \quad \Psi_{\pm} = \frac{A_{\oplus} B_y' \omega_g^2}{2[\omega_g^2 - \Delta_{\pm}^2]},$$

and $A_{1,2}$, C_{\pm} , D_{\pm} , E_{\pm} , and F_{\pm} are the undetermined coefficients.

It is seen that, besides the usual electromagnetic inductions in the local flat space-time, the perturbed electromagnetic fields induced by the GWs passing through the alternating magnetic field include three kinds of frequencies: ω_g and $\omega_g \pm \omega_B$. Distinguishing these signals from ones without any GW information provides an EM method of detection, rather than the mechanical one utilized in most current GW-detection setups like LIGO.

III. OBSERVABLE EFFECTS OF GW-INDUCED PERTURBED ELECTROMAGNETIC SIGNALS

We now investigate how to detect the GW-induced electromagnetic signals by distinguishing them for the ones related to the electrodynamics in flat space-time.

A. Transformation into the local coordinate system

It is well known that, in a curved space-time, only local measurements made by an observer traveling on a worldline are physical, and all observable quantities are just projections of the relevant tensors on the tetrads of the observer's worldline. Basically, the tetrads consist of three mutually orthogonal spacelike vectors and a timelike one. Thus, an observable $F_{(\alpha\beta)}$ measured by the observer can be expressed as the tetrad components of the relevant electromagnetic field tensor, i.e.,

$$F_{(\alpha\beta)} = F_{\mu\nu} \tau_{(\alpha)}^{\mu} \tau_{(\beta)}^{\nu}. \quad (14)$$

Obviously, for the present system the observer should be at rest in the static magnetic field, i.e., only the zeroth component of the four-velocity is nonvanishing. This implies that the tetrad $\tau_{(\alpha)}^{\mu}$ should have the form

$$\tau_{(0)}^{\mu} = (\tau_{(0)}^0, 0, 0, 0). \quad (15)$$

With the orthogonality of the tetrad $\eta_{\alpha\beta} = g_{\mu\nu}\tau_{(\alpha)}^\mu\tau_{(\beta)}^\nu$ and neglecting all the high-order small quantities, we have

$$\tau_{(\alpha)}^\mu = \begin{bmatrix} 1 & & & \\ & -1 - \frac{1}{2}h_\oplus & & \\ & h_\otimes & -1 - \frac{1}{2}h_\oplus & \\ & & & -1 \end{bmatrix}. \quad (16)$$

Consequently, the electromagnetic waves generated in the proposed GW probing system can be expressed as

$$E_{(x)} = cF_{(01)}, \quad E_{(y)} = cF_{(02)}, \quad E_{(z)} = cF_{(03)}, \quad (17)$$

with $F_{(0j)} = cF_{(\mu\nu)}\tau_{(0)}^\mu\tau_{(j)}^\nu$, $j = 1, 2, 3$, and

$$B_{(x)} = F_{(32)}, \quad B_{(y)} = F_{(13)}, \quad B_{(z)} = F_{(21)}. \quad (18)$$

Neglecting the second- and higher-order infinitely small terms $O(A_\otimes^2)$, we have

$$\begin{aligned} E_{(x)} = & \tilde{E}_x^{(0)} + \frac{i}{2}A_\oplus B_y^{(0)}\omega_g z \Lambda_{\omega_g}(z, t) \\ & + A_1 \Lambda_{\omega_g}(z, t) + A_2 \Lambda_{-\omega_g}(z, t) \\ & + i \sum_{\alpha=-,+} \alpha \Phi_{(\alpha)} \exp[i(k_g z - \Delta_\alpha t)] \\ & + \sum_{\alpha=-,+} \{C_\alpha \Lambda_{\Delta_\alpha}(z, t) + D_\alpha \Lambda_{-\Delta_\alpha}(z, t)\}, \quad (19) \end{aligned}$$

$$\begin{aligned} B_{(y)} = & B_y^{(0)} + B'_y \sin(\omega_B t) + \tilde{B}_y^{(0)} + \frac{i}{2}A_\oplus B_y^{(0)}k_g z \Lambda_{\omega_g}(z, t) \\ & + B_1 \Lambda_{\omega_g}(z, t) + B_2 \Lambda_{-\omega_g}(z, t) \\ & + i \sum_{\alpha=-,+} \alpha \Psi_{(\alpha)} \exp[i(k_g z - \Delta_\alpha t)] \\ & + \sum_{\alpha=-,+} \{E_\alpha \Lambda_{\Delta_\alpha}(z, t) + F_\alpha \Lambda_{-\Delta_\alpha}(z, t)\}. \quad (20) \end{aligned}$$

Above,

$$\begin{aligned} \Phi_{(\pm)} = \Phi_\pm &= \frac{A_\oplus B'_y \omega_g \Delta_\pm c}{2[\omega_g^2 - \Delta_\pm^2]}, \\ \Psi_{(\pm)} = \Psi_\pm - \frac{A_\oplus B'_y}{4} &= \frac{A_\oplus B'_y \omega_g^2}{2[\omega_g^2 - \Delta_\pm^2]} - \frac{A_\oplus B'_y}{4} \\ &= \frac{A_\oplus B'_y [\omega_g^2 + \Delta_\pm^2]}{4[\omega_g^2 - \Delta_\pm^2]}. \quad (21) \end{aligned}$$

Furthermore, with the simplified boundary conditions for the proposed configuration shown in Fig. 1:

$$\tilde{F}_{(\mu\nu)I}^{(1)}|_{z=0} = \tilde{F}_{(\mu\nu)II}^{(1)}|_{z=0}, \quad \tilde{F}_{(\mu\nu)II}^{(1)}|_{z=l} = \tilde{F}_{(\mu\nu)III}^{(1)}|_{z=l}, \quad (22)$$

the coefficients in Eqs. (12) and (13) can be obtained as

$$A_1 = A_2 = 0, \quad B_1 = B_2 = 0, \quad (23)$$

and

$$C_\pm = \mp i\Phi_{(\pm)}, \quad D_\pm = 0, \quad E_\pm = \mp i\Psi_{(\pm)}, \quad F_\pm = 0. \quad (24)$$

As a consequence, the distributions of the first-order perturbation electromagnetic fields can be further expressed as follows:

(a) In the region $z < 0$,

$$\tilde{E}_{(x)}^{(1)}(z, t) = \tilde{B}_{(y)}^{(1)}(z, t) = \tilde{E}'_{(x)}^{(1)}(z, t) = \tilde{B}'_{(y)}^{(1)}(z, t) = 0. \quad (25)$$

(b) In the region $0 < z < l$,

$$\begin{cases} \tilde{E}_{(x)}^{(1)}(z, t) = \frac{i}{2}A_\oplus B_y^{(0)}\omega_g z \Lambda_{\omega_g}(z, t), \\ \tilde{B}_{(y)}^{(1)}(z, t) = \tilde{E}_{(x)}^{(1)}/c, \end{cases} \quad (26)$$

and

$$\begin{cases} \tilde{E}'_{(x)}^{(1)}(z, t) = i \sum_{\alpha} \alpha \Phi_{(\alpha)} [\exp(-i\alpha\omega_B z) - 1] \Lambda_{\Delta_\alpha}(z, t), \\ \tilde{B}'_{(y)}^{(1)}(z, t) = i \sum_{\alpha} \alpha \Psi_{(\alpha)} [\exp(-i\alpha\omega_B z) - 1] \Lambda_{\Delta_\alpha}(z, t), \end{cases} \quad (27)$$

(c) In the region $z > l$,

$$\begin{cases} \tilde{E}_{(x)}^{(1)}(z, t) = \frac{i}{2}A_\oplus B_y^{(0)}\omega_g l \Lambda_{\omega_g}(z, t), \\ \tilde{B}_{(y)}^{(1)}(z, t) = \tilde{E}_{(x)}^{(1)}/c, \end{cases} \quad (28)$$

with $l = (2m + 1)\frac{\pi c}{\omega_B}$, $m = 0, 1, 2, \dots$, and

$$\begin{cases} \tilde{E}'_{(x)}^{(1)}(z, t) = -2i \sum_{\alpha} \alpha \Phi_{(\alpha)} \Lambda_{\Delta_\alpha}(z, t), \\ \tilde{B}'_{(y)}^{(1)}(z, t) = -2i \sum_{\alpha} \alpha \Psi_{(\alpha)} \Lambda_{\Delta_\alpha}(z, t), \end{cases} \quad (29)$$

As mentioned above, three kinds of electromagnetic signals could be generated as the GWs pass through the proposed semi-side transmission cavity biased by the alternating magnetic field $B_y(t)$. The first one is the zeroth-order perturbed electromagnetic signal with frequency ω_B , generated by the usual electromagnetic induction in the local flat space-time. It certainly does not carry any information about the passing GWs. The other ones are

originated from the perturbations of the GWs. Of course, various background sources of electromagnetic noise always exist, which should be filtered out by applying robust filter-wave techniques or suppressed by cleaning the system's environment.

B. Weak-light detections for the perturbation photon fluxes

Due to the small amplitude A_{\otimes} of the GW, the generated signals should be significantly weak. Physically, the average power densities $\langle S \rangle$, with $\langle S \rangle = \int_0^T S dt / T$, $\vec{S} = \vec{E} \times \vec{B} / \mu_0$, could be used to describe the strengths of various electromagnetic signals. Let us consider a detector in the z plane with a receiving area $x = [x_1, x_2]$, $y = [y_1, y_2]$, $x_1 = y_1 = -0.05$ m, $x_2 = y_2 = +0.05$ m, and thus an area $\Xi = 0.01$ m². Then, the average number of the photons with frequency ω detected per second can be calculated as

$$n = \frac{1}{\hbar\omega} \int_{x_1}^{x_2} \int_{y_1}^{y_2} \langle S \rangle dx dy, \quad (30)$$

with \hbar being Planck's constant, and

$$S = \frac{\tilde{E}_x(z, t) \tilde{B}_y(z, t)}{\mu_0} \simeq S^{(0)} + S_1^{(1)} + S_2^{(1)}. \quad (31)$$

Here, the zeroth-order perturbation energy flow density

$$\begin{aligned} S^{(0)} &= \frac{1}{\mu_0} (\tilde{E}_x^{(0)} \cdot \tilde{B}_y^{(0)}) \\ &= \frac{1}{4\mu_0} (B_y^{(0)})^2 c \sin^2 \left[\omega_B \left(\frac{z}{c} - t \right) \right] \end{aligned} \quad (32)$$

is generated by the usual electromagnetic induction of the alternating magnetic field $B_y(t)$, which could be treated as background noise. The corresponding average number of photons passing through a unit area is

$$n^{(0)} = \frac{\langle S^{(0)} \rangle_{\omega_B} \Xi}{\hbar\omega_B} = \frac{B_y'^2 c}{8\mu_0 \hbar \omega_B}. \quad (33)$$

It is certainly very large, compared with the first-order perturbation fields (which are proportional to the amplitude of GWs) with the energy flow densities

$$\begin{aligned} S_1^{(1)} &= \frac{1}{\mu_0} (\tilde{E}_x^{(0)} \cdot \tilde{B}_y^{(1)} + \tilde{E}_x^{(1)} \cdot \tilde{B}_y^{(0)}) \\ &= \frac{l B_y^{(0)} B_y'}{2\mu_0} A_{\oplus} \omega_g \sin \left[\omega_B \left(\frac{z}{c} - t \right) \right] \sin \left[\omega_g \left(\frac{z}{c} - t \right) \right] \end{aligned} \quad (34)$$

and

$$\begin{aligned} S_2^{(1)} &= \frac{1}{\mu_0} (\tilde{E}_x^{(0)} \cdot \tilde{B}_y^{(1)} + \tilde{E}_x^{(1)} \cdot \tilde{B}_y^{(0)}) \\ &= \frac{1}{\mu_0} \sum_{\alpha} [-\alpha (c\Psi_{(\alpha)} + \Phi_{(\alpha)})] B_y' \\ &\quad \times \sin \left[\omega_B \left(\frac{z}{c} - t \right) \right] \sin \left[\Delta_{\alpha} \left(\frac{z}{c} - t \right) \right], \end{aligned} \quad (35)$$

respectively. Obviously, if the GWs passing through the setup are resonant with the scanning local magnetic field, i.e., $\omega_g = \omega_B$, the perturbation photon flux with frequency ω_B ,

$$n_1^{(1)} = \frac{\langle S_1^{(1)} \rangle}{\hbar\omega_g} = \frac{B_y^{(0)} B_y' l \Xi}{4\mu_0 \hbar} A_{\oplus}, \quad (36)$$

can be generated simultaneously. Alternatively, if the frequencies of the GWs satisfy the condition $\omega_g = 2\omega_B$ (i.e., twice the frequency of the locally applied scanning alternating magnetic field), another kind of perturbation photon flux is also produced,

$$n_2^{(1)} = \frac{\langle S_2^{(1)} \rangle}{\hbar\omega_g} = \frac{3B_y'^2 c \Xi}{4\mu_0 \hbar \omega_g} A_{\oplus}. \quad (37)$$

To briefly summarize, the locally applied alternating magnetic field in the system simultaneously delivers three kinds of photon fluxes with the same frequency ω_B : the zeroth-order perturbation photons $n^{(0)}$ without any GW information, the first-order perturbation photons $n_1^{(1)}$ carrying GW information with frequency $\omega_g = \omega_B$, and the first-order perturbation photons $n_2^{(1)}$ carrying GW information with frequency $\omega_g = 2\omega_B$. This implies that, once the photon fluxes $n_1^{(1)}$ and $n_2^{(1)}$ are detected, the GWs with frequency $\omega_g = \omega_B$ or $\omega_g = 2\omega_B$ are probed correspondingly. Therefore, by scanning the frequency ω_B of the locally applied alternating magnetic field, the GWs signals with any reachable frequency (i.e., $\omega_g = \omega_B$ or $\omega_g = 2\omega_B$) can be probed simultaneously, if they actually exist.

Given that the intensities of the first-order perturbation photon fluxes (i.e., the signal photons) $n_1^{(1)}$ and $n_2^{(1)}$ are proportional to the amplitude A_{\oplus} of the GWs, they should be significantly less than the zeroth-order perturbation one, $n^{(0)}$. The question now is whether these significantly weak signals are still detectable. Specifically, Fig. 2 shows the detectable number of photons $n_1^{(1)}$ and $n_2^{(1)}$ versus the amplitude of the local alternating magnetic field B_y' , for GWs with the typical parameters $(A_{\oplus}, \omega_g) = (10^{-27}, 2\pi \times 10^8 \text{ Hz})$ and $(A_{\oplus}, \omega_g) = (10^{-29}, 2\pi \times 10^{10} \text{ Hz})$, respectively. Here, the generic argument $A_{\oplus} \propto \omega^{-1}$ [39] on the relation between the amplitude and frequency of the GWs is used. The applied static magnetic field is typically

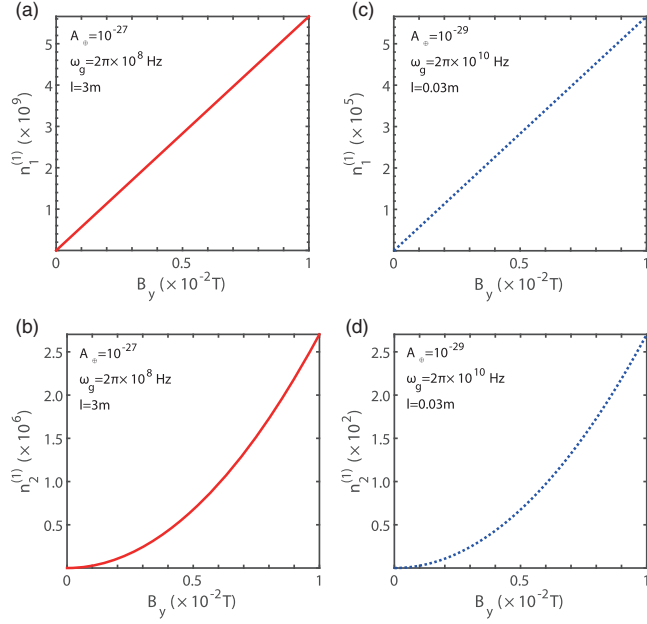


FIG. 2. Left: The detectable photon number of the first-order perturbation signals $n_1^{(1)}|_{\omega_B=\omega_g}$ (a), and $n_2^{(1)}|_{\omega_B=2\omega_g}$ (b) versus the amplitude B'_y , for the parameters $A_\oplus = 10^{-27}$, $\omega_g = 2\pi \times 10^8$ Hz, and $l = 3$ m. Right: The detectable photon number of the first-order perturbation signals $n_1^{(1)}|_{\omega_B=\omega_g}$ (c) and $n_2^{(1)}|_{\omega_B=2\omega_g}$ (d) versus the amplitude B'_y , for the parameters $A_\oplus = 10^{-29}$, $\omega_g = 2\pi \times 10^{10}$ Hz, and $l = 0.03$ m. Here, $B_y^{(0)} = 10$ T.

chosen as $B_y^{(0)} = 10$ T, which is achievable using current high-magnetic-field techniques, and the strength of the alternating magnetic field is set as $B'_y = [0, 1] \times 10^{-2}$ T. It is clear that without the alternating magnetic field (i.e., $B'_y = 0$) the detectable photons vanish (i.e., $n_1^{(1)} = n_2^{(1)} = 0$). The lower frequencies of the GWs correspond to stronger amplitudes of the GWs, and thus induce higher signal intensities. Additionally, the higher amplitudes of the alternating magnetic fields applied locally, yields the stronger electromagnetic responses of the GWs and consequently larger signal photon fluxes. The numerical results shown above indicate that the perturbation electromagnetic signals generated by the GWs passing through a locally biased high alternating magnetic field are strong enough to be detected by current weak-light detectors [32–35]. Thus, although the amplitude A_\oplus of the GWs is still significantly small, its induced photon fluxes with the present configuration are detectable, at least theoretically. Since the frequency of the applied locally alternating magnetic field is continuously adjustable, the system proposed here can be utilized to actively search for GWs within the achievable frequency band (typically the high-frequency one).

We emphasize that the proposed system for searching for GWs would work in a sufficiently wide band, as the

TABLE I. The detectable photon number of the first-order perturbation signals $n_1^{(1)}|_{\omega_B=\omega_g} = n_2^{(1)}|_{\omega_B=\omega_g}$ versus different kinds of GWs (A_\oplus, ω_g). The other parameters are chosen as $B_y^{(0)} = 10$ T and $B'_y = 0.005$ T.

A_\oplus	ω_B (Hz)	l (m)	$n_1^{(1)}$	$n_2^{(1)}$
10^{-26}	$2\pi \times 10^7$	30	2.83×10^{11}	6.76×10^7
10^{-27}	$2\pi \times 10^8$	3	2.83×10^9	6.76×10^5
10^{-28}	$2\pi \times 10^9$	0.3	2.83×10^7	6.76×10^3
10^{-29}	$2\pi \times 10^{10}$	0.03	2.83×10^5	67.6
10^{-30}	$2\pi \times 10^{11}$	3×10^{-3}	2.83×10^3	0.68
10^{-31}	$2\pi \times 10^{12}$	3×10^{-4}	28.3	0.07

frequency ω_B is adjustable within a very large range. Table I lists the typical frequency band of detectable GWs with the proposed configuration. One can see that the proposed setup should be able to probe GWs from 10^6 to 10^{12} Hz in cavities of these sizes.

Comparatively speaking, in the original GZ configuration (wherein the cavity is only biased by a time-independent high magnetic field) only the second-order perturbations of the GWs are delivered, and thus the corresponding perturbed EM signals are calculated as $\bar{E}_x^{(1)} = A_\oplus B^{(0)} k_g c z \exp[i(k_g z - \omega_g t)]$ and $\bar{B}_y^{(1)} = A_\oplus B^{(0)} k_g z \times \exp[i(k_g z - \omega_g t)]$. Here, $\bar{E}^{(1)}$ and $\bar{B}^{(1)}$ are parallel to the xy plane and perpendicular to each other [40,41]. As a consequence, in the terminal receiving area ($z = L$) the power flux density of this perturbed EMW can be estimated as

$$\bar{S} = \frac{1}{\mu_0} |\bar{E}_x^{(1)} \times \bar{B}_y^{(1)}| = \frac{1}{\mu_0} (A_\oplus B^{(0)} k_g L)^2 c, \quad (38)$$

which is linearly related to the square of the amplitude A_\oplus . For the same parameters used above ($A_\oplus = 10^{-27}$, $\omega_g = 2\pi \times 10^8$ Hz, $l = 3$ m, $B^{(0)} = 10$ T, and $\Xi = 0.01$ m²), the number of second-order perturbative photon signals is

$$\bar{n}^{(2)} = \frac{S\Xi}{\hbar\omega_g} \simeq 1.79 \times 10^{-14} \text{ s}^{-1}. \quad (39)$$

Obviously, these are very difficult to detect. Therefore, although the GZ effect is important for the detection of GWs, it is undetectable even with the current single-photon technique, while in the present configuration with the alternating high magnetic field the EMRs of the passing GWs are the first-order perturbation effects. The relevant perturbed signals, which are now proportional to the GW strain amplitude A_\oplus , are strong enough to be detected experimentally with the current weak-light detection techniques [32–36].

C. Filtering out the signals without GW information using the wave-impedance-matching technique

As we motioned above, the very strong zeroth-order EMWs generated by the usual electromagnetic inductions and the typically weak ones induced by the GW perturbations have the same frequency. This implies that the usual frequency matching filtering technique cannot be utilized to distinguish them. Indeed, with such a technique, all of the off-resonant EM signals (which are treated as the so-called background EM noise) with frequencies $\omega \neq \omega_B$ can be reflected and only the EM signals with the frequency $\omega_B = \omega_g$ are conducted into the detector. Given this, the next task for successful detection is to determine how to filter out the background photons (i.e., the resonant noise) without any GW information and conduct only the signal photons carrying GW information into the detector. Therefore, it is necessary to distinguish the three types of EM signals with the same frequency ω_B : the significantly strong zeroth-order perturbation photon fluxes $n^{(0)}$ (without any GW information), the first-order perturbation signal $n_1^{(1)}$ (carrying GW information with frequency $\omega_g = \omega_B$), and the first-order perturbation signal $n_2^{(1)}$ (carrying GW information with frequency $\omega_g = 2\omega_B$). This is how to filter out the unwanted signals $n^{(0)}$ and let only the those carrying GW information ($n_1^{(1)}$ and $n_2^{(1)}$) pass through to be detected.

Fortunately, another filtering technique, i.e., the so-called wave impedance matching, could be further utilized to effectively distinguish these three signals with the same frequency ω_B . Formally, the wave impedance of an electromagnetic wave is defined as the ratio of the transverse components of the electric and magnetic fields, i.e.,

$$Z = \frac{\mu E_x}{B_y}, \quad (40)$$

for a transverse-electric-magnetic plane wave traveling through a homogeneous medium μ . For the present configuration, the wave impedance of the zeroth-order perturbation signal with energy flow density $S^{(0)}$ generated by the local electromagnetic induction and satisfying the Maxwell equation in the flat space-time reads

$$Z_0 = \frac{\mu_0 E_x^{(0)}}{B_y^{(0)}} = \sqrt{\frac{\mu_0}{\epsilon_0}} \simeq 377 \, \Omega. \quad (41)$$

Here, ϵ_0 is the permittivity constant and μ_0 is the permeability constant in free space. However, the wave impedance of the first-order perturbed signal with energy flow density $S_1^{(1)}$ carrying GW information with frequency $\omega_g = \omega_B$ and obeying the Einstein-Maxwell equation in the curved space-time should be

$$Z_1^{(1)} = \frac{\mu_0 \tilde{E}_x^{(0)}}{\tilde{B}_x^{(1)}} = \frac{\mu_0 B'_y c^2}{B^{(0)} \omega_g l A_{\oplus}}, \quad (42)$$

or symmetrically,

$$Z_1'^{(1)} = \frac{\mu_0 \tilde{E}_x^{(1)}}{\tilde{B}_x^{(0)}} = \frac{\mu_0 B^{(0)} \omega_g l A_{\oplus}}{B'_y}. \quad (43)$$

They are strongly related to the frequencies and amplitudes of the resonant GWs. Similarly, the wave impedances of the first-order perturbed electromagnetic signals with energy flow density $S_2^{(1)}$ carrying GW information with frequency $\omega_g = 2\omega_B$ read

$$Z_2^{(1)} = \frac{\mu_0 \tilde{E}_x^{(0)}}{\tilde{B}'_{(y)}^{(1)}} = \frac{6\mu_0 c}{5A_{\oplus}} \quad (44)$$

and

$$Z_2'^{(1)} = \frac{\mu_0 \tilde{E}'_{(x)}^{(1)}}{\tilde{B}_y^{(0)}} = \frac{2\mu_0 A_{\oplus} c}{3}. \quad (45)$$

They are now independent of the frequencies of the resonant GWs.

Figure 3 shows how the wave impedances of the first-order perturbation signals depend on the GWs' parameters ω_g and A_{\oplus} . It is seen that the wave impedances of the first-order perturbation photon fluxes are significantly different from that of the zeroth-order perturbation one, i.e., $Z_1^{(1)}$, $Z_2^{(1)} \gg Z_0$; $Z_1'^{(1)}$, $Z_2'^{(1)} \ll Z_0$, respectively. This implies that, with the wave-impedance-matching technique, the electromagnetic signal $n^{(0)}$ without any GW information could be effectively filtered out. As a consequence, only the signals $n_1^{(1)}$ and $n_2^{(1)}$ carrying GW information could be conducted into the weak-light detectors. Therefore, detecting the first-order electromagnetic responses of the GWs passing through an alternating field is theoretically possible, although performing the relevant impedance-match filtering might be a great technical challenge.

D. Preliminary noise analysis

Noise suppression is always an important task in experimental measurements. Similarly, in the present configuration to probe the first-order electromagnetic responses of GWs passing through a cavity biased by an alternating magnetic field, various unavoidable sources of noise strongly limit the sensitivity of the detector and should be effectively suppressed. It is emphasized that—differing from the LIGO- and Virgo-type systems and the planned space-borne gravitational-wave detection programs to probe GWs in the low- and intermediate-frequency bands (wherein various *mechanical* sources of

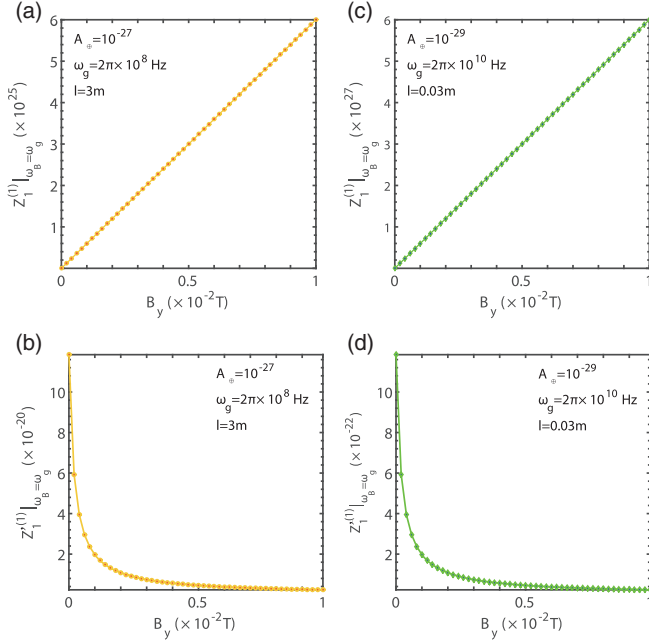


FIG. 3. The wave impedances of the first-order perturbation signals (a) $Z_1^{(1)}|_{\omega_B=\omega_g}$, (b) $Z_1^{(1)}|_{\omega_B=\omega_g}$, (c) $Z_2^{(1)}|_{\omega_B=\omega_g}$, and (d) $Z_2^{(1)}|_{\omega_B=\omega_g}$ versus the amplitude of the applied alternating magnetic field $B_y^{(0)}$ in a high magnetic field $B_y^{(0)} = 10$ T for typical frequencies and amplitudes of GWs: $(A_{\oplus}, \omega_g) = (10^{-27}, 2\pi \times 10^8 \text{ Hz})$ and $(10^{-29}, 2\pi \times 10^{10} \text{ Hz})$, respectively.

noise play relatively important roles)—the present configuration is disturbed mainly by various sources of *high-frequency EM noise*. The noise in the proposed system can be roughly divided into two categories: signal noise and detector noise. Signal noise refers to the background photons before detection and thus mainly includes i) thermal noise due to the nonzero environmental temperature (which yields a fluctuation of the length of the cavity biased by the magnetic field) and also the dark noise of the single-photon detector, ii) amplitude fluctuations of the applied magnetic field, iii) the frequency and phase noises of the applied alternating magnetic field, and iv) the zeroth-order perturbation photon flux $n^{(0)}$ due to the usual electromagnetic induction based on the usual flat space-time Maxwell theory. Certainly, thermal noise could be effectively suppressed by operating the system at ultra-low temperatures (i.e., millikelvins) for signal generation and detection by using well-developed superconducting single-photon detectors. The detector noise originates mainly from i) the limited quantum efficiency due to the signal loss during the single-detector coupling, ii) the limited readout time due to the various electronic relaxations in the readout circuits, and iii) the time jitters, etc.

Physically, the standard sensor designed for aggregating noise sources suggests that the noise for the system can be described by the noise-equivalent-power (NEP) parameter,

$$\text{NEP} = \sqrt{P_s^2 + P_d^2} = \sqrt{P_{tN}^2 + P_0^2 + P_{sn}^2 + P_{ob}^2}, \quad (46)$$

with P_s and P_d being the NEPs of the signal before detection and that in the detector, respectively. P_{tN} , P_0 , P_{sn} , and P_{ob} refer to the NEPs corresponding, respectively, to the thermal, zeroth-order electromagnetic induction, shot, and other background noises. As is well known, the thermal noise power

$$P_{tN} = 4k_B T \Delta f \quad (47)$$

(with bandwidth Δf) can be effectively neglected at ultra-low temperatures (e.g., in the millikelvin regime). With the usual frequency-matching filter with bandwidth $\Delta\omega_B$ related to that of the frequency fluctuation of the applied alternating magnetic field, almost all of the background electromagnetic noise P_{ob} outside the band $\omega_B \pm \Delta\omega_B$ can be neglected. The strongest noise P_0 originates from the electromagnetic induction of the applied alternating magnetic field, i.e., the zeroth-order response of the system, which does not carry any GW information. For the parameter selected in Table I (i.e., $B_y^{(0)} = 0.005$ T), such a power is estimated as $P_0 \sim 10^8$ W, which implies that the desired impedance-matching filter should have at least -80 dB attenuation for signals with a wave impedance of 377Ω . Finally, shot noise is inevitable and strongly influences the sensitivity of the single-photon detector used in current weak-signal detection methods. Basically, the maximum of the signal-to-noise ratio of the proposed system could be expressed as

$$(\text{SNR})_P = \frac{\eta}{2h\nu B} P_s = \frac{P_s}{\text{NEP}_{\min}},$$

with ν and P_s being the frequency and power of the signal, respectively. η and B are, respectively, the detection efficiency and band of the single-photon detector. As the band B is related to the integral time τ , i.e., $B = 1/(2\tau)$, the achievable minimum NEP of the detector is

$$\text{NEP}_{\min} = \frac{h\nu}{\tau\eta}.$$

Note that the NEP of the superconducting single-photon detector developed in the recent years [32,33,36] has reached about $10^{-20} \text{ W}/\sqrt{\text{Hz}}$, which implies that probing a single signal photon at the desired frequencies, e.g., 10^{12} Hz , within one second integral time is possible.

IV. CONCLUDING REMARKS

In summary, we proposed a theoretical technique to search for high-frequency GWs with a semi-open side cavity biased locally by an alternating high magnetic field. By analytically solving the Einstein-maxwell equation in

the curved space-time, the electromagnetic responses of the GWs passing through the cavity were obtained.

Certainly, the scheme proposed here to search for GWs by probing their EM responses is still too imprecise for realistic applications, in which various sources of noise and imperfect factors should be considered and the features of which should be precisely calibrated. Fortunately, in the present scheme for probing the high-frequency GWs, the usual sources of EM noise and shot noise are the main noise sources. Typically, the former could be effectively suppressed by the usual EM shielding. Also, although high-frequency EM noise directly influences the detected signals, we have shown that the usual frequency-matching and wave-impedance matching filtering techniques could be utilized to further suppress the high-frequency EM noise in the signals. In addition, the high-frequency signals we want

to detect are still sufficiently strong, and the remaining low-frequency EM and shot noise should be unimportant factors.

Anyway, the proposal provides an alternate approach to detecting GWs by probing their experimentally detectable EMRs with an alternating magnetic field. Hopefully, it could complement the very successful LIGO-Virgo detectors used to probe the mechanical tidal effects of GWs in the intermediate- and low-frequency bands.

ACKNOWLEDGMENTS

We thank Profs. Z. Y. Fang, X. G. Wu, and Z. B. Li for useful discussions. This work is partly supported by the National Natural Science Foundation of China (NSFC) under Grants No. U1330201 and No. 11174373.

-
- [1] See, e. g., M. Michele, *Gravitational Waves: Volume 1: Theory and Experiments* (Oxford University, New York, 2008).
- [2] B. P. Abbott *et al.*, *Phys. Rev. Lett.* **116**, 061102 (2016).
- [3] B. P. Abbott *et al.*, *Phys. Rev. Lett.* **116**, 241103 (2016).
- [4] B. P. Abbott *et al.*, *Phys. Rev. Lett.* **118**, 221101 (2017).
- [5] B. P. Abbott *et al.*, *Phys. Rev. Lett.* **119**, 141101 (2017).
- [6] B. P. Abbott *et al.*, *Phys. Rev. Lett.* **119**, 141101 (2017).
- [7] S. E. Whitcomb, *Classical Quantum Gravity* **10**, S185 (1993).
- [8] J. Aasi *et al.*, *Classical Quantum Gravity* **32**, 115012 (2015).
- [9] F. Acernese *et al.*, *Classical Quantum Gravity* **32**, 024001 (2015).
- [10] D. H. Douglass and V. B. Braginsky, in *General Relativity: An Einstein Centenary Survey*, edited by S. W. Hawking and W. Israel (Cambridge University Press, Cambridge, England, 2010), p. 98.
- [11] M. L. Tong and Y. Zhang, *Phys. Rev. D* **80**, 084022 (2009).
- [12] B. P. Abbott *et al.*, *Nature (London)* **460**, 990 (2009).
- [13] R.-G. Cai *et al.*, *Natl. Sci. Rev.* **4**, 687 (2017).
- [14] X. L. Fan, *Sci. China-Phys. Mech. Astron.* **59**, 640001 (2016).
- [15] R. A. Hulse and J. H. Taylor, *Astrophys. J.* **195**, L51 (1975).
- [16] J. H. Taylor and J. M. Weisberg, *Astrophys. J.* **253**, 908 (1982).
- [17] P. A. R. Ade *et al.*, *Phys. Rev. Lett.* **112**, 241101 (2014).
- [18] M. Canzoniere, E. Majorana, Y. Ogawa, P. Rapagnani, and F. Ricci, *Phys. Rev. D* **47**, 5233 (1993).
- [19] K. Danzmann and A. Rudiger, *Classical Quantum Gravity* **20**, S1 (2003).
- [20] D. Vetrugno *et al.*, *Int. J. Mod. Phys. D* **26**, 1741023 (2017).
- [21] M. Punturo *et al.*, *Classical Quantum Gravity* **27**, 194002 (2010).
- [22] B. S. Sathyaprakash, B. F. Schutz, and Van Den Broeck, *Classical Quantum Gravity* **27**, 215006 (2010).
- [23] B. S. Sathyaprakash *et al.*, *Classical Quantum Gravity* **30**, 079501 (2013).
- [24] S. Detweiler *et al.*, *Astrophys. J.* **234**, 1100 (1979).
- [25] R. W. Hellings and G. S. Downs, *Astrophys. J.* **265**, L39 (1983).
- [26] M. E. Gertsenshtein, *Sov. Phys. JETP Lett.* **14**, 84 (1962); Y. B. Zel'dovich, *Sov. Phys. JETP* **65**, 1311 (1973).
- [27] R. Ballantini, P. Bernard, E. Chiaveri, A. Chincarini, G. Gemme, R. Losito, R. Parodi, and E. Picasso, *Classical Quantum Gravity* **20**, 3505 (2003).
- [28] A. M. Cruise, *Classical Quantum Gravity* **20**, 3505 (2000).
- [29] A. M. Cruise and R. M. J. Ingle, *Classical Quantum Gravity* **22**, S479 (2005).
- [30] F.-Y. Li, M.-X. Tang, J. Luo, and Y.-C. Li, *Phys. Rev. D* **62**, 044018 (2000).
- [31] F.-Y. Li, M.-X. Tang, and D.-P. Shi, *Phys. Rev. D* **67**, 104008 (2003).
- [32] M. D. Eisamana, J. Fan, A. Migdall, and S. V. Polyakov, *Rev. Sci. Instrum.* **82**, 071101 (2011).
- [33] R. H. Hadfield, *Nat. Photonics* **3**, 696 (2009).
- [34] Y. Liang and H. P. Zeng, *Sci. China-Phys. Mech. Astron.* **57**, 1218 (2014).
- [35] X.-M. Li, L.-Y. Xie, and L. F. Wei, *Phys. Rev. A* **92**, 063840 (2015).
- [36] W. Guo, X. Liu, Y. Wang, Q. Wei, L. F. Wei, J. Hubmayr, J. Fowler, J. Ullom, L. Vale, M. R. Vissers, and J. Gao, *Appl. Phys. Lett.* **110**, 212601 (2017).
- [37] C. S. Kee, J.-E. Kim, H. Y. Park, and H. Lim, *IEEE Trans. Microwave Theory Tech.* **47**, 2148 (1999).
- [38] F.-Y. Li, H. Wen, Z.-Y. Fang, L.-F. Wei, Y.-W. Wang, and M. Zhang, *Nucl. Phys.* **B911**, 500 (2016).
- [39] K. S. Thorne, *Rev. Mod. Phys.* **52**, 285 (1980).
- [40] F. Y. Li, R. M. L. Baker, Z. Y. Fang, G. V. Stepheson, and Z. Y. Chen, *Eur. Phys. J. C* **56**, 407 (2008).
- [41] D. Boccaletti, V. De Sabbata, P. Fortini, and C. Gualdi, *Nuovo Cimento B* **70**, 129 (1970).